This article was downloaded by:
On: *14 January 2011*
Access details: *Access Details: Free Access*
Publisher *Taylor & Francis*
Informa Ltd Registered in England and Wales Registered Number: 1072954 Registered office: Mortimer House, 37-41 Mortimer Street, London W1T 3JH, UK

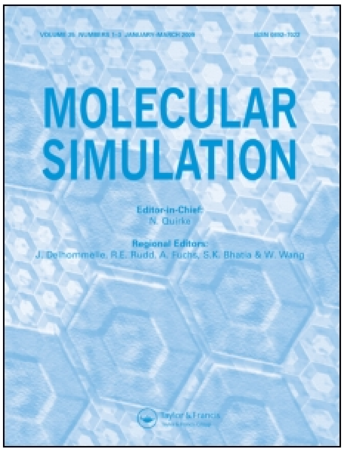

Molecular Simulation

Publication details, including instructions for authors and subscription information:
http://www.informaworld.com/smpp/title~content=t713644482

Spherical Boundary Conditions: A Finite and System Size Independent Geometry for Simulations of Electrolytic Liquids

Shabnam Hanassab[a]; T. J. VanderNoot[a]
[a] Chemistry Department, Queen Mary University of London, London, UK

Online publication date: 26 October 2010

To cite this Article Hanassab, Shabnam and VanderNoot, T. J.(2003) 'Spherical Boundary Conditions: A Finite and System Size Independent Geometry for Simulations of Electrolytic Liquids', Molecular Simulation, 29: 9, 527 — 533
To link to this Article: DOI: 10.1080/0892702031000152253
URL: http://dx.doi.org/10.1080/0892702031000152253

PLEASE SCROLL DOWN FOR ARTICLE

Full terms and conditions of use: http://www.informaworld.com/terms-and-conditions-of-access.pdf

This article may be used for research, teaching and private study purposes. Any substantial or systematic reproduction, re-distribution, re-selling, loan or sub-licensing, systematic supply or distribution in any form to anyone is expressly forbidden.

The publisher does not give any warranty express or implied or make any representation that the contents will be complete or accurate or up to date. The accuracy of any instructions, formulae and drug doses should be independently verified with primary sources. The publisher shall not be liable for any loss, actions, claims, proceedings, demand or costs or damages whatsoever or howsoever caused arising directly or indirectly in connection with or arising out of the use of this material.

Molecular Simulation, Vol. 29(9), September 2003, pp. 527–533

Taylor & Francis
Taylor & Francis Group

Spherical Boundary Conditions: A Finite and System Size Independent Geometry for Simulations of Electrolytic Liquids

SHABNAM HANASSAB* and T.J. VANDERNOOT†

Chemistry Department, Queen Mary University of London, Mile End Road, London E1 4NS, UK

(Received April 2003; In final form May 2003)

The system size dependence of the thermodynamic properties of electrolytic systems in "Spherical Boundary Conditions" (SBC) have been examined in this work. Coulombic systems were simulated with different system sizes (N) for a wide range of concentrations, different ionic charges and solvent permittivities. The effects of system size upon the mean internal energy $\langle U \rangle$ and mean ionic activity coefficient $\langle \gamma_{\pm} \rangle$ values were determined. Our results indicated that there was *no dependence* of the thermodynamic properties upon system size in the non-Euclidean geometry. Different methods of extrapolating the thermodynamic properties to infinite numbers were studied in detail. In contrast to the Euclidean geometry, the method of extrapolating $\langle U \rangle$ or $\langle \gamma_{\pm} \rangle$ versus N^{-1}, $N^{-2/3}$ and $N^{-1/3}$ was not statistically justifiable nor advantageous.

Therefore, SBC is well suited to simulating systems involving long-range electrostatic interactions because the results do not dependent upon system size.

Keywords: Non-Euclidean; Geometry; Monte Carlo simulations; Spherical Boundary Conditions; Hypersphere and Electrolytes

INTRODUCTION

The determination of thermodynamic and structural properties of electrolytic solutions by computer simulations has been a subject of substantial research within the past few decades [1–43]. Because computer simulations provide information about the properties of a microscopic system, this system should be simulated in geometry which has the minimum effect on these properties and at the same time is consistent with properties of the macroscopic system. The simulation of Coulombic systems has the additional complication that the ion–ion interactions are quite long-ranged.

The Euclidean geometry, which is a cubic geometry, has been used for most computations of Coulombic systems [5–28,33–43]. This geometry is always accompanied by "Periodic Boundary Conditions" (PBC) in order to overcome the problem of the box boundaries and to avoid an interface with vacuum. The majority of the groups, who studied electrolytic systems by means of simulations, had used Ewald summation in order to deal with long-ranged electrostatic interactions. This method was originally developed for lattice problems and consequently that can make it lees suitable for application in the simulations of disordered or interfacial systems. A detailed discussion of the disadvantages of using Ewald summation for the simulation of electrolytic liquids has been given by Valleau and Whittington [44]. There have been only a few attempts to develop alternatives to the Ewald method for simulations in which long-ranged interactions are involved. However, these new methods can introduce their own disadvantages [45–51]. Therefore, the problem of having a suitable geometry in simulations of electrolytic solutions has remained unresolved.

An alternative geometry and boundary condition was suggested by Isenberg in 1973. Isenberg suggested using the 3D surface of a 4D hypersphere for simulations. This geometry is a non-Euclidean geometry with "Spherical Boundary Conditions" (SBC). Hansen *et al.* [52] used this geometry in simulating a 2D electron gas within a neutralising uniform background continuum charge on the 2D

---

*E-mail: s.hanassab@qmul.ac.uk.
†Corresponding author. E-mail: tjv@cognitrix.com

ISSN 0892-7022 print/ISSN 1029-0435 online © 2003 Taylor & Francis Ltd
DOI: 10.1080/0892702031000152253

surface of a sphere. Since then, some groups [29–32,52–60] have used SBC in their simulations, but there have been some limitations, as we discussed elsewhere [1].

In our previous works [1,2] we reported Monte Carlo simulations of Restricted Primitive Model (RPM) and Primitive Model (PM) electrolytes in a non-Euclidean geometry. That work was successful and we indicated that SBC was a very good alternative for simulations of disordered electrolytic systems. A main advantage that we found with that geometry was that the thermodynamic and structural properties showed a very weak system size dependence.

The groups who have studied the system size dependence of the cubic geometry with PBC, have tried to find the best way of extrapolating the mean internal energies and the mean ionic activity coefficients to infinite numbers [5–7]. For instance Sloth and Sørensen [5] have studied this and they concluded that for electrolytes it was best to extrapolate the internal energy against the reciprocal of the total system size (N), and the mean ionic activity coefficient versus $N^{-1/3}$. Elsewhere, Sørensen [30] has explained and discussed the strong dependence of the thermodynamic properties on system size. This dependence was most pronounced for dilute systems and Sørensen [30] concluded that the best way to plot the internal energy was to extrapolate it versus $N^{-2/3}$ and there are similar discussions about the extrapolation of mean ionic activity coefficient to infinite numbers [5–7]. However, no explanation was given in order to explain why various methods of extrapolation should make a significant different in presenting the results nor why researchers should examine this issue.

Card and Valleau [15] simulated a range of system sizes at two different concentrations and found a noticeable N dependence in the values of mean internal energy. However, Card and Valleau used the minimum image convention [15] in their work and that could be a source of complications in their simulations of electrolytes. Caillol [29] simulated the RPM model as bicharged spheres in non-Euclidean geometries and concluded that for a 1:1 electrolyte the mean activity coefficient depended linearly upon N^{-1}. However, Caillol [29] has not discussed whether this system size dependence may be due to either using bicharges or the geometry which was used in the simulations.

In this work, we studied the system size dependence of the thermodynamic quantities of electrolytes in non-Elucildean geometries. We studied the effect of system size on the thermodynamic properties as a factor of solvent permittivity for 1:1 and 2:2 electrolytes at different concentrations. We also report the values of mean internal energy and the mean ionic activity coefficient for a range of system sizes, ionic charges and concentrations of 0.001 M (as a dilute system) to 1.00 M (as a concentrated system), in order to study different methods of extrapolation.

METHOD

The 3D hyperspherical MC simulations in canonical ensemble are presented here. The program which was described previously was used in this work as well (all the details are given in previous work [1–2]). We carried out simulations of 1:1, 1:3, 2:2, 2:3, 3:1, 3:2 and 3:3 electrolytes using SBC geometry over a range of concentrations, solvent permittivities and system sizes (number of the particles) at room temperature (300 K). The solvent permittivities that we used in this work were: $\varepsilon = 10-78.4$ for 1:1 electrolytes and $\varepsilon = 40-78.4$ for 2:2 electrolytic system (the reason for this latter range was to avoid any cases of crystallisation as we discussed and explained elsewhere [1]). We use ionic radii of $r_{\pm} = 250$ pm as in the previous work, because it is a reasonable ionic radius for the simulations of solvated 1:1 and 2:2 RPM electrolytes. For any other charge combinations we used a PM model, using the calculated hydrodynamic ionic radii (Table I) [2] for the ions. The data were analysed in EasyPlot 4 and Origin 6.

RESULTS AND DISCUSSION

The sets of simulations were run for 1:1 and 2:2 electrolytes for a range of system sizes from $N = 40-500$ for concentrations of 0.001–1.00 M. Figure 1a is an example graph of internal energy versus concentration (for a 2:2 electrolyte). The mean internal energy decreased as the concentration

TABLE I The average hydrodynamic radii of some typical cations and anions in each charge group were calculated from the molar conductivities of those particular ions reported in the literature using the formula [61]: $r_i = z^2F^2/6\pi N_A\lambda_i^o\eta$ where r_i is the hydrodynamic radius of an ion (*i.e.* the radius of the ion including the hydration shell), z is the integral charge of the ion, F is the Faraday, N_A is Avogadro's constant, λ_i^o is the molar conductivity of the ion and η is the viscosity of the solvent. Notice that in this way the mean hydrodynamic radius for each particular charge represents an average over typical values for ions of that charge. The mean value was taken and used as a typical anionic or cationic radius in the simulations of electrolytes with asymmetric charges.

z	*Average Hydrodynamic Radius/pm*
+ 1	200
+ 2	650
+ 3	1200
− 1	140
− 2	500
− 3	900

increased and this was due to the stronger electrostatic interactions as the ions became closer to one another at higher concentrations. The fact that all the data points were so closely clustered at each concentration suggested that there was no obvious system size dependence. There were slight variations at higher concentrations for different system sizes, but at the same time the uncertainties were higher for smaller system sizes and the points were not statistically significantly different (Fig. 1b). The weighted linear least squares fit showed that there was no statistically significant slope, because the standard error of the slope was actually higher than the slope itself. Similar behaviour was observed for 1:1 electrolytes, when we analysed the data for the mean internal energy. The mean ionic activity coefficient also showed no number dependence for 1:1 and 2:2 charges over a range of concentrations.

The effect of number dependence on the thermodynamic properties of the system was studied, as a function of charge, concentration and solvent permittivities. Figure 2a and 2b show the mean internal energies versus the reduced Bjerrum value (B^*), which represents the charge and permittivity, for a range of system sizes from $N = 40-300$, for 0.001 and 1.00 M, respectively. The mean internal energy decreased as B^* increased (i.e. increase in charge and/or decreases in permittivity). However, there was no significant system size dependence observed in the results. There were some statistical variations for the mean internal energy at higher B^* for different system sizes. But there were no trends for these values and the uncertainties were larger than at lower B^* values. This was due to the fact that a higher B^* values, where the solvent permittivity was lower, the systems with smaller populations of ions had more freedom in movement. Mean ionic activity coefficients showed similar behaviour to

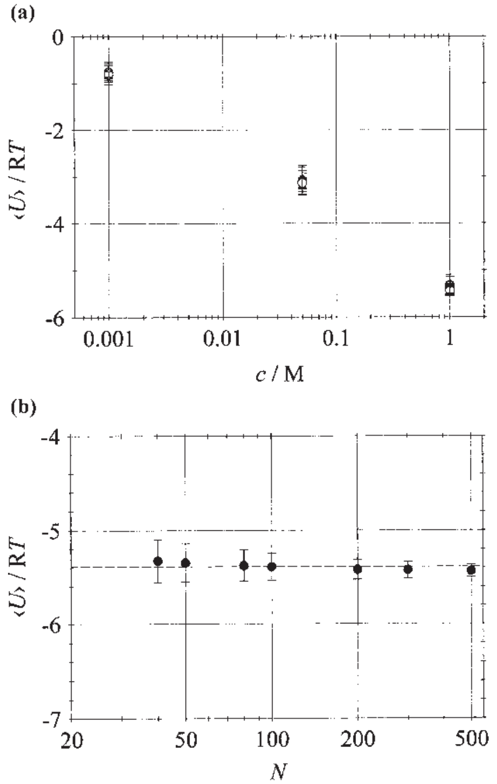

FIGURE 1 (a) Reduced mean internal energy, $\langle U\rangle/RT$, as a function of concentration (c) for a range of particle numbers $N = 40-500$. The conditions of the simulations were: $T = 300\,\mathrm{K}$, $\varepsilon = 78.4$, $q_i = \pm 2$ and $r_\pm = 250\,\mathrm{pm}$. A single standard deviation is indicated on our data by the error bars. Notice that the points at each concentration almost overlap indicating a very weak system size dependence. (b) Reduced mean internal energy, $\langle U\rangle/RT$ versus N at 1.00 M. The conditions of the simulations were: $T = 300\,\mathrm{K}$, $\varepsilon = 78.4$, $q_i = \pm 2$ and $r_\pm = 250\,\mathrm{pm}$. A single standard deviation is indicated on our data by the error bars. Notice that the uncertainties are higher at smaller system sizes. From the weighted linear least squares fit the value of the slope is: $-1.418 \times 10^{-4} \pm 2.447 \times 10^{-4}$, which indicates that the slope is not statistically different from zero. The error from the weighted linear least squares fit is given as standard error. The dashed line indicates the mean of the data points.

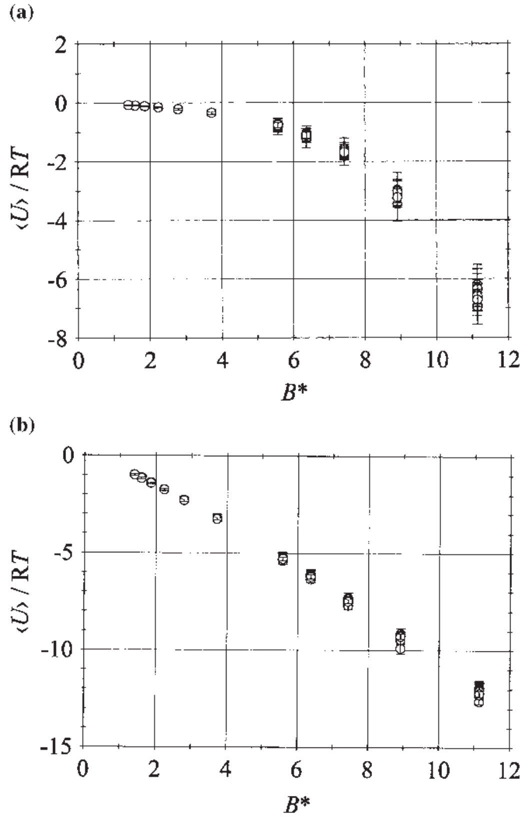

FIGURE 2 Mean internal energy, $\langle U\rangle$ normalised by RT, as a function of reduced Bjerrum parameter (B^*) defined as: $B = z_+ z_- e^2/8\pi\varepsilon_0\varepsilon r_\pm k_\mathrm{B}T$ where z_+ and z_- are the integral charge of the ions, e is the charge of an electron, ϵ_0 is the permittivity of free space, ϵ is the relative permittivity (dielectric constant), r_+ and $r_-$are the radii of the ions, k_B is the Boltzmann constant and T (K) is the temperature of the system. The Bjerrum parameter represents the charge and permittivity, for a range of $N = 40-300$. The simulation conditions were: $T = 300\,\mathrm{K}$, $\varepsilon = 10-78.4$, $q_i = \pm 1$ and ± 2 and $r_\pm = 250\,\mathrm{pm}$. A single standard deviation is indicated on our data by the error bars. (a) $c = 0.001\,\mathrm{M}$ and (b) $c = 1.00\,\mathrm{M}$.

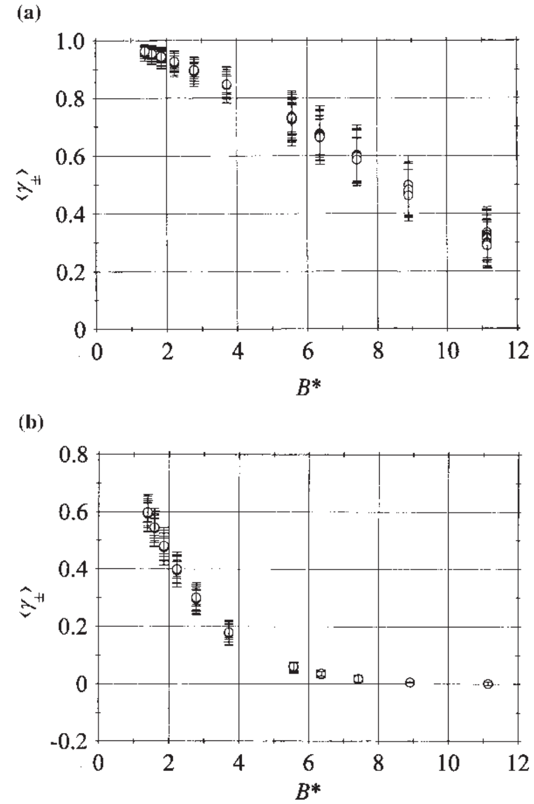

FIGURE 3 Mean ionic activity coefficient $\langle\gamma_\pm\rangle$, as a function of the reduced Bjerrum value (B^*), which characterizes the charge and permittivity, for a range of $N = 40{-}300$. The simulation conditions were: $T = 300\,\mathrm{K}$, $\varepsilon = 10{-}78.4$, $q_i = \pm 1$ and ± 2 and $r_\pm = 250\,\mathrm{pm}$. A single standard deviation is displayed on our data by the error bars. (a) $c = 0.001\,\mathrm{M}$ and (b) $c = 1.00\,\mathrm{M}$.

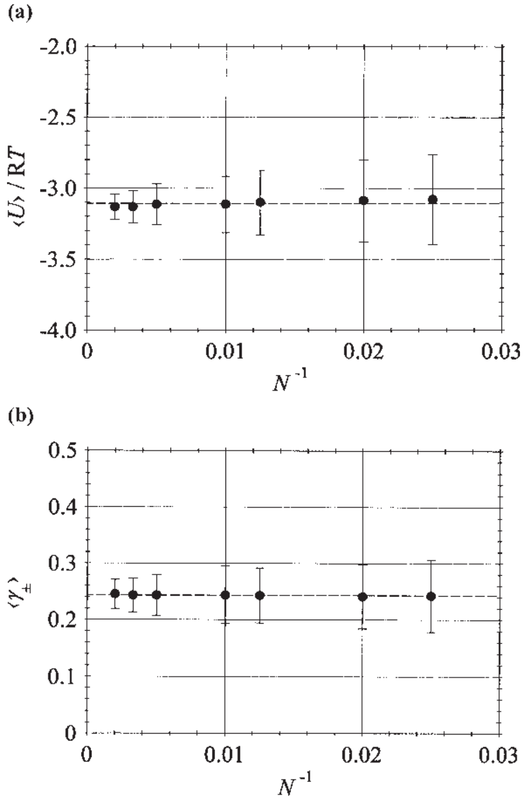

FIGURE 4 (a) Reduced mean internal energy, $\langle U\rangle/RT$ plotted as a function of N^{-1}. The simulation conditions were: $T = 300\,\mathrm{K}$, $\varepsilon = 78.4$, $q_\pm = \pm 2$, $r_\pm = 250\,\mathrm{pm}$ and $c = 0.05\,\mathrm{M}$. A single standard deviation from the simulation is indicated on our data by the error bars. The circles show the data from the simulation. The dashed line indicates the mean of the data points. (b) $\langle\gamma_\pm\rangle$ as a function of N^{-1} for a 2:2 electrolyte. The simulation conditions were: $T = 300\,\mathrm{K}$, $\varepsilon = 78.4$, $r_\pm = 250\,\mathrm{pm}$ and $c = 0.05\,\mathrm{M}$. A single standard deviation is marked on our data by the error bars. The circles show the data from the simulation and the dashed line indicates the mean of the data points.

mean internal energies, meaning that $\langle\gamma_\pm\rangle$ decreased as B^* increased for both concentrations. The data points at the higher values of B^* were checked by plotting the internal energy versus the reciprocal of the system size and the weighted linear least squares fit indicated that there was no statistical variation. Figure 3a and 3b indicate there was no obvious system size dependence in the case of different charges or solvent permittivities in SBC. There were some variations in the values of mean ionic activity coefficients at higher B^*, and the reason for that was the same as that discussed for the mean internal energies.

In the final section, we tested the different methods of extrapolating system size dependence as has been discussed in the literature. This type of extrapolation may be important where one needs to account for the effect of system size on the thermodynamic properties. The mean internal energies and the ionic activity coefficients were plotted versus N^{-1}, $N^{-2/3}$ and $N^{-1/3}$ for all the charge combinations in a range of concentrations. We used a system size range of $N = 40{-}500$. We then did a weighted linear least squares fit for each of our 42 graphs. From the fits for each set of N^{-1}, $N^{-2/3}$ and $N^{-1/3}$ we analysed the quality of the curve fit (r^2) and the slopes to determine if different methods of extrapolation would affect the results significantly. The examples of these graphs for $\langle U\rangle$ and $\langle\gamma_\pm\rangle$ for 2:2 electrolytes at 0.05 M are shown in Figure 4a and 4b. We also tabulated our results of these extrapolations for 1:1, 2:2 and 2:3 electrolytic systems at different

TABLE II Mean internal energy versus number for various charge combinations. The value of the slope and the standard error from the weighted linear least squares fit for each specific graph are shown. The simulation conditions were: $T = 300\,\mathrm{K}$, $\varepsilon = 78.4$, $c = 0.001\,\mathrm{M}$ and $r_\pm = 250\,\mathrm{pm}$ for 1:1 and 2:2 electrolytes and the radii of the ions for 2:3 charges are as given in Table I.

Charge	*x-axis*	α (*Slope*)	*se* (α)
1:1	$N^{-1/3}$	− 0.030	0.154
1:1	$N^{-2/3}$	− 0.078	0.393
1:1	N^{-1}	− 0.254	1.257
2:2	$N^{-1/3}$	0.208	0.878
2:2	$N^{-2/3}$	0.536	2.255
2:2	N^{-1}	1.688	7.282
2:3	$N^{-1/3}$	0.255	1.472
2:3	$N^{-2/3}$	0.690	3.772
2:3	N^{-1}	2.290	12.138

TABLE III Mean ionic activity coefficients versus the system size for various charge combinations. The value of the slope from the weighted least squares fit for each specific graph is shown. The simulation conditions were: $T = 300\,\mathrm{K}$, $\varepsilon = 78.4$, $c = 0.001\,\mathrm{M}$ and $r_{\pm} = 250\,\mathrm{pm}$ for 1:1 and 2:2 electrolytes and the radii of the ions for 2:3 charges are as given in Table I. The standard error of the weighted linear least squares curve fits are shown.

Charge	*x-axis*	α (*Slope*)	*se* (α)
1:1	$N^{-1/3}$	-0.033	0.131
1:1	$N^{-2/3}$	-0.082	0.328
1:1	N^{-1}	-0.256	1.035
2:2	$N^{-1/3}$	0.055	0.436
2:2	$N^{-2/3}$	0.138	1.080
2:2	N^{-1}	0.427	3.378
2:3	$N^{-1/3}$	-0.023	0.339
2:3	$N^{-2/3}$	-0.052	0.854
2:3	N^{-1}	-0.148	2.710

TABLE IV Mean internal energy versus number for 1:1 and 2:2 electrolytes at $c = 1.00\,\mathrm{M}$. The value of the slope from the weighted linear least squares fit for each specific graph is shown in the table. The simulation conditions were: $T = 300\,\mathrm{K}$, $\varepsilon = 78.4$, and $r_{\pm} = 250\,\mathrm{pm}$. The standard error of the linear curve fits are also shown in this table.

Charge	*x-axis*	α (*Slope*)	*se* (α)
1:1	$N^{-1/3}$	0.08	0.428
1:1	$N^{-2/3}$	0.215	1.096
1:1	N^{-1}	0.708	3.525
2:2	$N^{-1/3}$	0.602	0.890
2:2	$N^{-2/3}$	1.557	2.278
2:2	N^{-1}	4.987	7.322

TABLE V Mean ionic activity coefficients versus number for 1:1 and 2:2 electrolytes at $c = 1.00\,\mathrm{M}$. The value of the slope from the weighted linear least squares fit for each specific graph is shown in the table. The simulation conditions were: $T = 300\,\mathrm{K}$, $\varepsilon = 78.4$ and $r_{\pm} = 250\,\mathrm{pm}$. The standard error of the linear curve fits are presented on this table too.

Charge	*x-axis*	α (*Slope*)	*se* (α)
1:1	$N^{-1/3}$	-0.049	0.278
1:1	$N^{-2/3}$	-0.119	0.705
1:1	N^{-1}	-0.362	2.245
2:2	$N^{-1/3}$	-0.032	0.091
2:2	$N^{-2/3}$	-0.075	0.226
2:2	N^{-1}	-0.218	0.706

TABLE VI Mean internal energy versus number for 2:2 electrolytes at $c = 0.05\,\mathrm{M}$. The value of the slope from the linear curve fit for each specific graph is shown in the table. The simulation conditions were: $T = 300\,\mathrm{K}$, $\varepsilon = 78.4$ and $r_{\pm} = 250\,\mathrm{pm}$. The standard error of the weighted linear least squares fits are shown here too.

Charge	*x-axis*	α (*Slope*)	*se* (α)
2:2	$N^{-1/3}$	0.307	1.234
2:2	$N^{-2/3}$	0.789	3.160
2:2	N^{-1}	2.510	10.168

TABLE VII Mean ionic activity coefficients versus number for 2:2 electrolytes at $c = 0.05\,\mathrm{M}$. The value of the slope from the linear fit for each specific graph is shown in the table. The simulation conditions were: $T = 300\,\mathrm{K}$, $\varepsilon = 78.4$ and $r_{\pm} = 250\,\mathrm{pm}$. The standard error of the weighted linear least squares fits are shown.

Charge	*x-axis*	α (*Slope*)	*se* (α)
2:2	$N^{-1/3}$	-0.018	0.283
2:2	$N^{-2/3}$	-0.043	0.707
2:2	N^{-1}	-0.130	2.227

TABLE VIII Mean internal energy versus number for 2:3 electrolytes at $c = 0.02\,\mathrm{M}$. The value of the slope from the weighted linear fit for each specific graph is shown in the table. The simulations conditions were: $T = 300\,\mathrm{K}$, $\varepsilon = 78.4$ and the radii of the ions were as given in Table I. The standard error of the weighted linear least squares fit are shown in this table.

Charge	*x-axis*	α (*Slope*)	*se* (α)
2:3	$N^{-1/3}$	1.430	1.499
2:3	$N^{-2/3}$	3.485	3.838
2:3	N^{-1}	10.571	12.342

TABLE IX Mean ionic activity coefficients versus number for 2:3 electrolytes at $c = 0.02\,\mathrm{M}$. The value of the slope from the linear weighted least square fit for each specific graph is shown in the table. The simulation conditions were: $T = 300\,\mathrm{K}$, $01\varepsilon = 78.4$ and the radii of the ions were as indicated in Table I. The standard error of the linear fits are also shown in this table.

Charge	*x-axis*	α (*Slope*)	*se*(α)
2:3	$N^{-1/3}$	-0.035	0.335
2:3	$N^{-2/3}$	-0.079	0.837
2:3	N^{-1}	-0.217	2.632

concentrations (Table II–IX). For each plot we did a weighted linear least squares fit and obtained the value of slope, which had an error higher than the actual value of the slope. This means that there is no statistical dependence of $\langle U\rangle/\mathrm{R}T$ and $\langle\gamma_{\pm}\rangle$ upon different system sizes. The details of our results with other charge combinations are not given here, but our results indicated that there was no system size dependence for any of them either.

We concluded that the slopes were statistically equal to zero regardless of the method of extrapolation. Therefore, no extrapolation is preferred to another one and in fact extrapolation is not necessary. In this work, we have investigated this effect very carefully. SBC is well suited for simulations of the Coulombic systems. For a system as small as 100 ions it was possible to achieve results which were in good agreement with macroscopic systems [2]. This is a very good feature of SBC, because with less computational effort, reliable results can be obtained.

CONCLUSIONS

SBC is a finite geometry, which is well suited for simulations of electrolytic solutions, because the thermodynamic quantities show *no dependence* upon system size.

References

[1] Hanassab, S. and VanderNoot, T.J. (2002) "Monte Carlo simulations of restricted primitive model (RPM) electrolytes in non-Euclidean geometries", *J. Electroanal. Chem.* **528**, 135.

[2] Hanassab, S. and VanderNoot, T.J. (2003) "Monte Carlo simulations of primitive model (PM) electrolytes in non-Euclidean geometries", *J. Electroanal. Chem.*, Submitted.

[3] VanderNoot, T.J. (2000) "Factors affecting the calculations of mean ionic activities in Monte Carlo simulations of primitive model electrolytes", *PCCP.* **2**, 253.

[4] VanderNoot, T.J. and Panayi, A. (1998) "Monte Carlo simulations of restricted primitive electrolytes in a 2D non-Euclidean geometry", *J. Chem. Soc. Faraday Trans.* **94**, 1939.

[5] Sloth, P. and Sørensen, T.S. (1998) "Monte Carlo simulations of single-ion chemical potentials: Preliminary results for the restricted primitive model", *Chem. Phys. Lett.* **143**, 140.

[6] Sørensen, S. (1990) "How wrong is the Debye–Huckel approximation for dilute primitive model electrolytes with moderate Bjerrum parameter", *J. Chem. Soc. Faraday Trans.* **86**, 1815.

[7] Sloth, P. and Sørensen, T.S. (1988) "Monte Carlo simulations of single ion chemical potentials: Results for the unrestricted primitive model", *Chem. Phys. Lett.* **146**, 452.

[8] Sloth, P. (1992) "Electrochemical potentials in the grand canonical ensemble: Some formal and numerical results for confined ionic systems", *Mol. Phys.* **77**, 667.

[9] Sloth, P. and Sørensen, T.S. (1990) "Monte Carlo calculations of chemical potentials in ionic fluids by application of Widom's formula: Correction for finite-system effects", *Chem. Phys. Lett.* **173**, 51.

[10] Sloth, P. and Sørensen, T.S. (1990) "Single-ion activity coefficients and structure of ionic fluids. Results for the primitive model of electrolyte solutions", *J. Chem. Phys.* **94**, 2116.

[11] Sørensen, T.S. (1993) "Direct calculation of the electric potential distributions around ions from high precision canonical ensemble Monte Carlo simulations of some primitive model electrolyte system", *Mol. Simul.* **11**, 267.

[12] Sloth, P., Sørensen, T.S. and Jensen, J.B. (1987) "Monte Carlo calculations of thermodynamic properties of the restricted, primitive model of electrolytes at extreme dilution using 32, 44, 64, 100, 216 and 512 ions and *ca.* 10^6 configurations per simulation", *J. Chem. Soc. Faraday Trans.* **2**(83), 881.

[13] Sloth, P. (1992) "Electrochemical potentials in the grand canonical ensemble: Some formal and numerical results for confined ionic systems", *Mol. Phys.* **77**, 667.

[14] Sørensen, T.S. (1991) "Error in the Debye–Huckel approximation for dilute primitive model electrolytes with Bjerrum parameters of 2 and *ca.* 6.8 investigated by Monte Carlo methods", *J. Chem. Soc. Faraday Trans.* **87**, 479.

[15] Card, D.N. and Valleau, J.P. (1970) "Monte Carlo study of the thermodynamic of electrolyte solutions", *J. Chem. Phys.* **52**, 6232.

[16] Hummer, G. and Soumpasis, D.M. (1993) "The correlations and free energies in restricted primitive model descriptions of electrolytes", *J. Chem. Phys.* **98**, 581.

[17] Valleau, J.P., Cohen, L.K. and Card, D.N. (1980) "Primitive model electrolytes. II. The symmetrical electrolyte", *J. Chem. Phys.* **72**, 5942.

[18] Vlachy, V., Ichiye, T. and Haymet, A.D.J. (1991) "Symmetric associating electrolytes: GCMC simulations and integral equation theory", *J. Am. Chem. Soc.* **113**, 1077.

[19] Rasaiah, J.C., Card, D.N. and Valleau, J.P. (1972) "Calculations on the restricted primitive model for 1:1 electrolyte solutions", *J. Chem. Phys.* **56**, 248.

[20] Lyubartsev, A.P., Martsinovski, A.A. and Shevkunov, S.V. (1992) "New approach to Monte Carlo calculation of the free energy: Method of expanded ensemble", *J. Chem. Phys.* **96**, 1776.

[21] Larsen, B. (1976) "Studies in statistical mechanics of Coulombic systems. I. Equation of state for the restricted primitive model", *J. Chem. Phys.* **65**, 3431.

[22] Bresme, F. and Abascal, J.L.F. (1993) "Pair connectedness functions and percolation in highly charged electrolyte solutions", *J. Chem. Phys.* **99**, 9037.

[23] Bresme, F., Lomba, E., Weis, J.J. and Abascal, J.L.F. (1995) "Monte Carlo simulation and integral-equation studies of a fluid of charged hard spheres near the critical region", *Phys. Rev. E.* **51**, 289.

[24] Vega, C., Bresme, F. and Abascal, J.L.F. (1996) "Fluid–solid equilibrium of a charged hard-sphere model", *Phys. Rev. E* **54**, 2746.

[25] Van Megan, W. and Snook, I.K. (1980) "The grand canonical ensemble Monte Carlo method applied to electrolyte solutions", *Mol. Phys.* **39**, 1043.

[26] Torrie, G.M. and Valleau, J.P. (1980) "Electrical double layers. I. Monte Carlo study of a uniformly charged surface", *J. Chem. Phys.* **73**, 5807.

[27] Valleau, J.P. and Card, D.N. (1972) "Monte Carlo estimation of the free energy by mutistage sampling", *J. Chem. Phys.* **57**, 5457.

[28] Rogde, S.A. and Hafskjold, B. (1983) "Equilibrium properties of a 2:2 electrolyte model. Monte Carlo and integral equation results for the restricted primitive model", *Mol. Phys.* **48**, 1241.

[29] Caillol, J.M. (1993) "A new potential for the numerical simulations of electrolyte solutions on a hypersphere", *J. Chem. Phys.* **99**, 8953.

[30] Caillol, J.M. and Weis, J.J. (1995) "Free energy and cluster structure in the coexistence region of the restricted primitive model", *J. Chem. Phys.* **102**, 7610.

[31] Caillol, J.M. (1994) "A Monte Carlo study of the liquid–vapour coexistence of charged hard spheres", *J. Chem. Phys.* **100**, 2161.

[32] Weis, J.J., Levesque, D. and Caillol, J.M. (1998) "Restricted primitive model of an ionic solution confined to a plane", *J. Chem. Phys.* **109**, 7486.

[33] Sevensson, B.R. and Woodward, C.E. (1988) "Widom's method for uniform and non-uniform electrolyte solutions", *Mol. Phys.* **64**, 247.

[34] Karaska, T. (1997) "The structure and volume of ion cluster in the restricted primitive model", *Mol. Phys.* **90**, 165.

[35] Pitzer, K.S. and Schreiber, D.R. (1987) "The restricted primitive model for ionic fluids, properties of the vapour and the critical region", *Mol. Phys.* **60**, 1067.

[36] Valleau, J.P. and Cohen, L.K. (1980) "Primitive model electrolytes. I. Grand canonical Monte Carlo computations", *J. Chem. Phys.* **72**, 5935.

[37] Sevensson, B.R. and Woodward, C.E. (1988) "Widom's method for uniform and non-uniform electrolyte solutions", *Mol. Phys.* **64**, 247.

[38] Liano-Restrepo, M. and Chapman, W.G. (1994) "Monte Carlo simulation of the structural properties of concentrated aqueous alkali halide solutions at 25°C using a simple civilized model", *J. Chem. Phys.* **100**, 8321.

[39] Rogde, S.A. (1983) "Monte Carlo results for an electrolyte-solution model. Divalent charged hard-spheres of unequal diameter", *Chem. Phys. Lett.* **103**, 133.

[40] Sevensson, B., Akesson, T. and Woodward, C.E. (1991) "On the simulation of thermodynamic and structural properties of simple liquids", *J. Chem. Phys.* **95**, 2717.

[41] Rasaiah, J.C. (1972) "Computations for higher valence electrolytes in the restricted primitive model", *J. Chem. Phys.* **56**, 3071.

[42] Abramo, M.C., Caccamo, C., Malescio, G., Pizzimenti, G. and Rogde, S.A. (1984) "Equilibrium properties of charged hard spheres of different diameters in the electrolyte solution regime: Monte Carlo and integral equation results", *J. Chem. Phys.* **80**, 4396.

[43] Corti, H.R., Laria, D. and Trevani, L.N. (1996) "Ionic association in asymmetric electrolytes", *J. Chem. Soc. Faraday Trans.* **92**, 91.

[44] Valleau, J.P. and Whittington, S.G. (1977) "A guide to Monte Carlo for statistical mechanics: 1. Highways", *Statistical Mechanics. A. A Modern Theoretical Chemistry* (B.J. Berne, New York), pp 137–168.

[45] Barker, J.A. and Watts, R.O. (1973) "Monte Carlo studies of the dielectric properties of water-like models", *Mol. Phys.* **26**, 789.

[46] Friedman, H.L. (1975) "Image approximation to the reaction field", *Mol. Phys.* **29**, 1533.

[47] Neumann, M., Steinhauser, O. and Pawley, G.S. (1984) "Consistent calculation of the static and frequency dependent dielectric constant in computer simulations", *Mol. Phys.* **52**, 97.

[48] Wang, L. and Herman, J. (1995) "Reaction field molecular dynamics simulation with Friedman's image charge method", *J. Phys. Chem.* **99**, 12001.

[49] Nymand, T.M. and Linse, P. (2000) "Ewald Summation and reaction field methods for potentials with atomic charges, dipoles and polarizabilities", *J. Chem. Phys.* **112**, 6152.

[50] Nymand, T.M. and Linse, P. (2000) "Molecular dynamics simulations of polarizable water at different boundary conditions", *J. Chem. Phys.* **112**, 6386.

[51] Sloth, P. and Sørensen, T.S. (1992) "Hard charged spheres in spherical pores. Grand canonical ensemble Monte Carlo calculations", *J. Chem. Phys.* **96**, 548.

[52] Hansen, J.P., Levesque, D. and Weis, J.J. (1979) "Self-diffusion in the two-dimensional, classic electron gas", *Phys. Rev. Lett.* **43**, 979.

[53] Kratky, K.W. (1980) "New boundary conditions for computer experiments of thermodynamic systems", *J. Comp. Phys.* **37**, 205.

[54] Kratky, K.W. and Schreiner, W. (1982) "Computational techniques for spherical boundary conditions", *J. Comp. Phys.* **47**, 313.

[55] Caillol, J.M. and Levesque, D. (1991) "Numerical simulations of homogeneous and inhomogeneous ionic systems: An efficient alternative to the Ewald method", *J. Chem. Phys.* **94**, 597.

[56] Caillol, J.M. and Levesque, D. (1992) "Structural, thermodynamic and electrical properties of polar fluids and ionic-solutions on a hypersphere: Results of simulations", *J. Chem. Phys.* **96**, 1477.

[57] Caillol, J.M. (1993) "Search of the gas–liquid transition of dipolar hard spheres", *J. Chem. Phys.* **98**, 9835.

[58] Caillol, J.M. (1992) "Structural, thermodynamic and electrical properties of polar fluids and ionic solutions on a hypersphere: theoretical aspects", *J. Chem. Phys.* **96**, 1455.

[59] Delville, A., Pelleng, R.J-M. and Caillol, J.M. (1997) "A Monte Carlo (NVT) study of the stability of charged interfaces: A simulation on a hypersphere", *J. Chem. Phys.* **106**, 7275.

[60] Caillol, J.M. (1999) "Numerical simulations of Coulomb systems: A comparison between hyperspherical and periodic boundary conditions", *J. Chem. Phys.* **111**, 6528.

[61] Hibbert, D.B. (1993) *Introduction to Elecrochemistry*, 1st ed. (Macmillan, UK), p 113.